REPORT DOCUMENTATION PAGE

Form Approved
OMB No. 0704-0188

1. REPORT DATE *(DD-MM-YYYY)*	2. REPORT TYPE	3. DATES COVERED *(From - To)*
19 October 2006	Final Report	4 April 2002 - 30 September 2004

4. TITLE AND SUBTITLE

Concluding Analysis of IR Measurements of Microbreaking and Whitecaps

5a. CONTRACT NUMBER

5b. GRANT NUMBER

N00014-02-1-0523

5c. PROGRAM ELEMENT NUMBER

6. AUTHOR(S)

Andrew T. Jessup
Ruth Branch

5d. PROJECT NUMBER

5e. TASK NUMBER

5f. WORK UNIT NUMBER

7. PERFORMING ORGANIZATION NAME(S) AND ADDRESS(ES)

Applied Physics Laboratory - University of Washington
1013 NE 40th Street
Seattle, WA 98105-6698

8. PERFORMING ORGANIZATION REPORT NUMBER

9. SPONSORING/MONITORING AGENCY NAME(S) AND ADDRESS(ES)

Office of Naval Research (322PO)
875 North Randolph Street, Suite 1425
Arlington, VA 22203-1995

10. SPONSOR/MONITOR'S ACRONYM(S)

ONR

11. SPONSOR/MONITOR'S REPORT NUMBER(S)

12. DISTRIBUTION/AVAILABILITY STATEMENT

Approved for public release

13. SUPPLEMENTARY NOTES

14. ABSTRACT

Analysis of existing field and laboratory measurements using infrared techniques to study wave breaking was conducted by studying skin temperature modulation by microbreaking waves and correlation of microbreaking with radar backscatter. The field data were from the Fluxes, Air-sea Interaction, and Remotes Sensinf or FAIRS, Experiment that took place off Monterey, CA in fall 2000. Laboratory results were taken at the NASA Goddard Wallops Flight Facility in 1998 and 2004.

15. SUBJECT TERMS

Infrared, microbreaking, wave breaking, IR imagery, swell modulation, modulation transfer function, microwave

16. SECURITY CLASSIFICATION OF:			17. LIMITATION OF ABSTRACT	18. NUMBER OF PAGES	19a. NAME OF RESPONSIBLE PERSON
a. REPORT	b. ABSTRACT	c. THIS PAGE			Andrew Jessup
Unclassified	Unclassified	Unclassified	UU		19b. TELEPHONE NUMBER *(Include area code)* 206-685-2609

Final Report: ONR Award N00014-02-0523
Concluding Analysis of IR Measurements of Microbreaking and Whitecaps
04 Apr 2002 through 30 Sep 2004

Andrew T. Jessup
Applied Physics Laboratory, University of Washington
1013 NE 40th St., Seattle, WA 98105-6698
jessup@apl.washington.edu, 206-685-2609

OBJECTIVE

Analysis of existing field and laboratory measurements using infrared techniques to study wave breaking was concluded by accomplishing the two tasks described below. The field data were from the Fluxes, Air-sea Interaction, and Remote Sensing, or FAIRS, Experiment that took place off Monterey, CA in fall 2000. The laboratory data were taken at the NASA Goddard Wallops Flight Facility in 1998 and 2004.

RESEARCH TASKS

Task 1: Skin Temperature Modulation by Microbreaking Waves

One of the goals for FAIRS was to use IR imagery to determine the extent to which microbreaking waves are modulated by swell. In 1998 and 2004, we made laboratory measurements using an IR imager of wind-generated waves superimposed on paddle-generated waves. The laboratory results suggested that modulation of the skin temperature observed in the field was due to modulation of microbreaking by swell waves.

Task 2: Correlation of Microbreaking with Radar Backscatter

Gravity-capillary waves bound to the forward face of swell waves have been postulated to be the cause of large Doppler shifts in radar backscatter at high incidence angles. To investigate the relationship between these bound scatterers and microbreakers, we made simultaneous, co-located IR, video, and radar measurements during FAIRS. Microbreakers were identified as waves which produced a warm wake in the IR imagery but no visible signature in the video. The large Doppler shift in the radar data associated with these waves supports the idea that microbreaking waves are a source of bound scatterers in radar return from the ocean.

DELIVERABLES

Under this award, Ruth Fogelberg completed her MS thesis on comparison of the IR and microwave signatures of breaking waves [*Fogelberg*, 2003]. A manuscript was submitted to the IEEE Transactions on Geosciences and Remote Sensing covering these results. In the review process, the editor recommended submitting a shorter version on the IR results alone, which we have done [*Branch and Jessup*, 2006]. For the purposes of this final report, we have attached the original manuscript since it covers both the IR and microwave results.

Branch, R. and A. T. Jessup, Infrared Signatures of Microscale Wave Breaking Modulation, IEEE Geoscience and Remote Sensing Letters, submitted, 2006.

Fogelberg, R. A., A study of microbreaking modulation by ocean swell using infrared and microwave techniques, M.S. thesis, Univ. of Wash., Seattle, 129 pp, 2003.

Infrared and Microwave Signatures of Microbreaking Waves and Their Modulation

Ruth Branch, Andrew T. Jessup, *Member, IEEE,* William J. Plant, *Member, IEEE,* Martin Gade, *Member, IEEE*

Abstract— **Infrared and microwave signatures of microbreaking waves and their modulation by swell waves were investigated in ocean and laboratory experiments. Simultaneous collocated infrared and microwave measurements of wind waves and swell on the ocean were made and compared with infrared measurements of wind waves and paddle-generated waves in the laboratory. On the ocean, the skin temperature, T_{skin}, and the normalized radar cross section, σ_0, were both modulated by the swell, but with differing phases. In general, T_{skin} maxima occurred on the rear face of the swell while σ_0 maxima occurred on the front face. Infrared imagery from the ocean and laboratory showed that swell-induced microbreaking occurred at or near the swell crest and that the resulting warm wakes occurred on the rear face of the wave. When tilt and range modulation are taken into account, the location of microbreaking also accounts for the maximum of σ_0 occurring on the front face of the swell. Thus, microbreaking waves generated near the crest of low-amplitude swell can produce IR and microwave signatures with the observed phase. The relationship between IR and microwave modulation was further emphasized by comparing IR and visible images of the sea surface with simultaneous microwave Doppler spectra from the same spot. When small and microscale breaking waves were present, Doppler spectra exhibited characteristics similar to those from whitecaps, having peaks with large Doppler offset and polarization ratios near unity. When no microbreakers were present, Doppler offsets and polarization ratios were much smaller in accordance with composite surface scattering theory.**

Index Terms—**microbreaking, swell modulation, infrared, microwave, ocean surface waves, wave breaking, modulation transfer function**

I. Introduction

Modulation of sea surface temperature and microwave backscatter by swell waves has been observed on the ocean, but the mechanisms responsible for the phenomena are not completely understood. Furthermore, the extent to which the mechanisms that cause temperature modulation are related to those for backscatter modulation is unknown. Here we use simultaneous infrared (IR), and microwave measurements from the ocean and IR measurements from the laboratory to examine the relationship between temperature and backscatter modulation by swell waves.

The surface temperature measured by an IR radiometer corresponds to the so-called skin temperature, T_{skin}, because the ocean thermal boundary, or skin, layer is O(1 mm) thick and the IR optical depth is O(10 μm). T_{skin} within the wake of a breaking wave is approximately equal to the bulk temperature, T_{bulk}, because the breaking process mixes water from below to the surface [1,2]. Thus, the skin temperature modulation due to breaking can be observed because T_{skin} inside the breaking wake area is different from T_{skin} outside the area. Modulation of T_{skin} by swell waves has been observed on the ocean [3, 4] and in the laboratory [5, 6]. On the ocean, *Jessup and Hesany* [4] (hereafter JH) found that the magnitude of the T_{skin} modulation was of the same order as the bulk-skin temperature difference, $\Delta T = T_{bulk}-T_{skin}$, and that the maximum T_{skin} occurred on the forward face of the swell crest at a phase ψ of 90° (relative to the crest at ψ=0°). JH suggested that small-scale wave breaking due to longwave/shortwave interaction might explain their observations. *Wick and Jessup* [7] simulated and tested several mechanisms proposed to explain T_{skin} modulation and concluded that preferential breaking of small-scale waves best explained the observations of JH. They found that when the preferential breaking was placed on the forward face of swell waves at a phase of 90°, the maximum modulation occurred at ψ=45°.

Modulation of microwave backscatter by swell waves is a well known phenomenon [8] and is composed of range, tilt, and hydrodynamic modulation [9]. Range and tilt modulation are due to the change in distance and orientation between the sensor and the surface as a wave propagates through the field-of-view (FOV). Hydrodynamic modulation characterizes how the wave number power spectrum is affected along the profile of swell waves. Weak hydrodynamic interaction theory predicts that the maximum modulation of small-to-intermediate gravity waves will occur near the crest of the swell, whereas capillary waves will be enhanced on the forward face near ψ=90° [10]. Hara and Plant [11] showed that tilt and range modulations shift the maximum of

Manuscript received May 8, 2006. This work was supported in part by the Office of Naval Research.

R. Branch was with the Applied Physics Laboratory, University of Washington, Seattle, WA 98105 USA. She is now at the University of Cape Town, Cape Town, South Africa (e-mail: ruth.branch@gmail.com).

A. T. Jessup and W. J. Plant are with the Applied Physics Laboratory, University of Washington, Seattle, WA 98105 USA. (e-mail: jessup@apl.washington.edu, plant@apl.washington.edu).

M. Gade is with the Center for Marine and Climate Research, University of Hamburg, Hamburg, Germany. (e-mail: gade@ifm.uni-hamburg.de)

measured microwave modulations about 45° farther toward the front face of the swell when it propagates toward the microwave antenna. *Plant* [12] developed a model to explain characteristics of the Doppler spectrum of microwave backscatter at large incidence angles by including Bragg scattering from bound, tilted waves. He proposed that in addition to the modulated capillary and gravity-capillary waves, gravity waves with wavelength O(1m) may be modulated sufficiently by the swell to generate shorter waves bound to them. He postulated that this occurs on the forward face of the swell at ψ=130°. These short gravity waves with bound, tilted shorter waves are reminiscent of microbreaking waves [13], which are short gravity waves that break without entraining air. Microbreaking waves have a bore-like crest with parasitic capillary waves that ride along on the forward face and have been shown to produce an IR signature caused by disruption of the skin layer [14-16]. Thus a primary motivation of this work was to determine if the microwave scatterers proposed by *Plant* [12] at ψ=130° are related to microbreaking that causes T_{skin} modulation.

II. Ocean Measurements

IR and microwave scatterometer data were acquired during the Fluxes, Air-sea Interaction, and Remote Sensing, or FAIRS, Experiment on the R/P FLIP in the Fall of 2000. An IR imager, IR radiometer, K_u-band microwave scatterometer, and a video camera were mounted on booms over the water and positioned with collocated fields of view. The scatterometer was mounted at an incidence angle of 70° and the IR instruments at 33°. The sensors were pointed into the wind and remained so for the entire experiment since FLIP was freely floating. A full description of the experiment can be found in [17].

The time series in Fig. 1 illustrate the modulation of σ_{VV} and σ_{HH}, the normalized radar cross sections at vertical and horizontal polarizations, respectively, and T_{skin}. The T_{skin} data are from the IR radiometer and correspond to the average temperature over a spot on the surface of roughly 30 cm in diameter. The surface displacement, η, is superimposed as a dashed line on the other times series. The swell and wind waves were aligned. The power spectra of T_{skin}, σ_{VV}, and σ_{HH} in Fig. 2 exhibit strong peaks at the swell frequency. In general, the maximum temperature appears on the rear face of the swell waves while cross section maxima occur on the front face. The occurrence of the maximum radar cross section on the front face is consistent with previous observations. However, the location of the temperature maxima on the rear face is inconsistent with the observation of the maxima on the front face reported by JH. We will argue that this may be due to the different conditions occurring in the two experiments.

The two main criteria for observing significant modulation of T_{skin} are large ΔT and large wave height. In practice, this translates into conditions of low wind speed and large swell, since ΔT is largest at low wind speed where swell provides the only significant surface displacements. The dependence of the modulation on ΔT is illustrated in Fig. 3, which shows time series from FAIRS of ΔT and the linear transfer function, $H(f_o)$, between T_{skin} and η evaluated at the swell frequency f_o. In this case, a decrease in wind speed from above 5 m s^{-1} to below 2 m s^{-1} led to a steady increase in ΔT and a concordant increase in $H(f_o)$. A large ΔT was present only occasionally during the FAIRS experiment and occurred mostly when the swell was small, resulting in a limited number of cases of significant T_{skin} modulation. The scatter plot of significant wave height versus wind speed in Fig. 4 illustrates the difference in wind and wave conditions during FAIRS compared to those during the JH measurements. During FAIRS, the waves were locally generated, so that large wave heights were accompanied by high winds and therefore small ΔT. The conditions during the observations made by JH were ideal for significant T_{skin} modulation because remarkably large, long period swell waves were present for several days under light winds. Below, we will discuss how these differing conditions could explain the different phases of the temperature modulation observed during the two experiments.

Although the environmental conditions during FAIRS were not generally conducive to T_{skin} modulation, direct observations of the generation of microbreaking waves by swell were made with the use of an IR imager. In the time series of IR images in Fig. 5, the crest of a swell wave propagating down the image induces microbreaking. The microbreakers are numbered when they first appear and leave behind warm wakes that are easily tracked. Note that the breaking begins at or near the swell crest and the wakes grow and remain present on the back side of the crest. The swell has propagated almost out of the field of view by the last image and several warm wakes are visible on the surface.

The sequence of images in Fig. 5 provides insight into the relationship between microbreaking and T_{skin} modulation. A radiometer time series corresponding to the imagery in Fig. 5 would probably not exhibit significant T_{skin} modulation because of the relatively low density of events. Although the breaking events in Fig. 5 appear to begin at or near the swell crest, the skin temperature in the wakes left behind by the breaking process remains elevated for a significant period after the swell crest has passed. In general, the phase of the T_{skin} modulation at a point will be a function of the location of the breaking relative to the crest, the phase speed of the crest, and the time that it takes the skin layer to recover after a disruption. The skin layer recovery time can range from several seconds at low wind speeds, as in Fig. 5, to 0.1 s at high wind speeds [18]. If the recovery time is a significant fraction of the swell period, then T_{skin} where a microbreaker occurs will remain elevated while the surface displacement continues to vary.

The association of whitecaps and large amplitude excursions in the radar cross section, or sea spikes, in moderate incidence angle measurements is well established [19, 20] and continues to be an area of active research [21-23]. Characteristics of backscatter associated with sea spikes due to breaking waves include a polarization ratio, σ_{HH}/σ_{VV}, near unity, a large Doppler frequency shift, and

increased Doppler bandwidth [19]. The microwave signature of breaking over a wide range of scales is illustrated in Fig. 6 by comparing Doppler spectra for VV and HH polarization with simultaneous, collocated IR and video imagery. The case of backscatter from the sea surface without wave breaking is shown in Fig. 6a, in which the dotted ellipse on the IR image indicates the scatterometer's approximate field of view. In the absence of breaking, the Doppler spectra is characterized by $\sigma_{HH}/\sigma_{VV}<1$ and symmetric peaks with a small offset. The whitecap in Fig. 6b, which appears warm in the IR image, produces a Doppler spectrum with $\sigma_{HH}/\sigma_{VV}\approx1$ at higher frequencies, and a mean Doppler shift significantly greater than zero. The spectrum also shows significant return near zero frequency with $\sigma_{HH}/\sigma_{VV}<1$, which corresponds to backscatter from the surface not affected by breaking. The white crest in the IR image is an apparent temperature increase due to the increased emissivity of foam [2]. The Doppler spectra from the much smaller whitecap shown in the IR sequence and video image in Fig. 6c are remarkably similar to those from the large whitecap in Fig. 6b. The final example is an IR image sequence in Fig. 6d showing the wake of a microbreaking wave, outlined by a dashed circle, that propagates through the images in time. Although the video image shows no visible signature, the Doppler spectra show significant return with a large mean frequency, and $\sigma_{HH}/\sigma_{VV}\approx1$. This example, as well as other similar events observed during FAIRS, demonstrates that microbreaking waves produce microwave backscatter with characteristics similar to those from whitecaps.

III. Laboratory Measurements

The discrepancy between the phase of the T_{skin} modulation reported by JH and that observed during FAIRS led us to perform a laboratory experiment in which we could combine wind waves and swell (paddle-generated waves) under controlled conditions. The experiment was conducted in the wind-wave tank at the Air-Sea Interaction Research Facility at the Wallops Flight Facility of the NASA Goddard Space Flight Center [24], which is capable of producing both wind waves and paddle-generated waves. The wind-wave flume is 18.3 m long, 1.2 m high, and 0.9 m wide. The water depth was 0.76 m, the head space was 0.46 m, and the measurements were made at a fetch of approximately 9 m. A video camera, IR imager, and IR radiometer were used to view the water surface.

The two image sequences in Fig. 7 compare the IR signature of microbreaking wind waves with and without the paddle-generated waves present. In the case of wind waves alone in Fig. 7a, individual warm wakes of microbreakers appear to be randomly distributed over the image. When both wind and swell waves are present as in Fig. 7b, the swell crest appears as a bright horizontal band caused by microbreaking occurring uniformly across the image. This example clearly demonstrates how the swell causes preferential breaking of the wind waves near its crest.

Modulation of T_{skin} by the swell waves is also apparent in the time series and power spectra from a point measurement of temperature. The time series of T_{skin} in Fig. 8 was calculated from the average pixel value along a horizontal line across the image. The T_{skin} and η time series show that the temperature maxima tend to appear on the rear face of the swell. The times when microbreaking was observed at the wave gauge location are indicated on the η time series by black dots. Microbreaker crests were individually detected by thresholding the IR images and performing a gradient operation. Although a detectable microbreaking wave was not present at every swell crest, the dots indicate that the breaking generally occurred at those crests. The inset IR images correspond to maxima or minima in the T_{skin} time series and include a horizontal line marking the location of the radiometer spot. The coincident IR imagery shows that breaking occurs near the swell crest and that the T_{skin} maxima occur when the warm wake of a microbreaker passes through the radiometer footprint. Minima in the time series correspond to times when the warm wake has propagated past the radiometer footprint and T_{skin} is the undisturbed surface temperature. The phase between T_{skin} and η specifies where the warm wakes are with respect to the swell but not where the microbreaking occurs.

In the laboratory, microbreaking preferentially occurred at the swell crest and the T_{skin} maxima occurred on the back face due to persistence of the warm wake left behind by the breaking. These findings are consistent with the FAIRS result that the T_{skin} maxima from the radiometer occurred on the rear face of the crest. They are also consistent with the FAIRS IR imagery, which showed breaking occurring at the crest and warm wakes on the back side.

IV. Phase Discrepancy of Temperature Modulations

The laboratory measurements strongly indicate that the FAIRS IR results are valid, but they do not resolve the difference between the FAIRS and JH measurements, where the T_{skin} maxima occurred on the front face at $\psi=90°$. We offer two possible explanations for this discrepancy.

The first explanation is that another mechanism besides preferential breaking might have been responsible for the modulation observed by JH. As noted above, the wind and wave conditions during JH were significantly different than during FAIRS, which suggests the possibility that a different mechanism may dominate depending on the conditions. In addition to the preferential microbreaking, Wick and Jessup [7] considered the effect of enhanced wind stress and heat flux due to the air flow over the swell waves. They found that a variety of parameterizations of ΔT [25-27] in terms of friction velocity and heat flux resulted in modulation of T_{skin} with $\psi=180°$ and magnitudes that were comparable to the observations for some but not all wind speeds. Specifically, ΔT parameterizations by *Wick et al.* [26] and *Fairall et al.* [27] predicted scattered but reasonable magnitudes for wind speeds between 1.5 m s^{-1} and 5 m s^{-1} but magnitudes that were too low for higher or lower wind speeds. The difference in predicted versus observed phase combined with the limited wind speed range and the scatter led Wick and Jessup [7] to conclude that enhanced wind stress was likely not responsible for the

JH results. However, the wind stress enhancement they considered did not include the effect of the skin layer recovery time and swell phase speed, which we have shown can introduce a phase shift between the location of a surface disruption and its manifestation as an increase in T_{skin}. Since the effect is to reduce the phase, the predicted phase of 180° (trough) due to enhanced wind stress would be reduced to a value corresponding to a location on the forward face, as observed by JH.

A second possible explanation of the discrepancy between the FAIRS and JH temperature modulation phases rests on the very different amplitudes of the modulating swell. Plant's [12] hypothesis was that the swell modulates all waves that were much shorter than its wavelength. If the modulation was sufficiently strong, gravity waves on the order of a meter long could be sufficiently steepened that they begin to break at a location other than the crest of the swell. Thus two regions of strong microwave scattering could exist along the swell wave so that the resulting modulation is a combination of the two. Since Plant required that the region where meter-length waves break must lie well forward of the swell crest, temperature signatures generated there would also appear well in front of the crest. These would strengthen as the swell amplitude increased, explaining their presence in the JH measurements and absence in the FAIRS data. Additional research is necessary to determine whether either of these possible explanations is correct.

Recently, Zappa et al. [28] reported on field measurements of skin temperature modulation. They found that the phase of the modulation shifted from the front to the rear face of the swell as the wind speed changed from low to high. They suggested that the reason was the change in the relative occurrence of large-scale and microscale breaking. Under low winds the modulation was dominated by microbreaking occurring on the forward swell face. Under high winds, the modulation was dominated by large-scale breaking occurring at the swell crest. These results are consistent with our suggestion that the phase of the modulation depends on environmental conditions, specifically changes in the wind conditions and the type and location of breaking.

V. Conclusion

Modulation of sea surface temperature and microwave backscatter by swell waves was investigated using ocean and laboratory observations. The presence of T_{skin} modulation is dependent on the wave height, the bulk-skin temperature difference, the density of microbreaking waves, the phase speed of the swell, and the skin layer recovery time. On the ocean, radar cross section maxima occurred on the forward face of the swell traveling toward the antenna while the T_{skin} maxima occurred on the rear face. The microwave results were consistent with previous investigations but the IR measurements disagreed with the results of Jessup and Hesany [4], who found T_{skin} maxima on the forward face. IR imagery showed that modulation of microbreaking waves was present even when their density was not high enough to modulate T_{skin} measured by a radiometer. Furthermore, the imagery showed that the swell-induced breaking occurred at or near the swell crest and that the resulting warm wakes occurred and persisted on the rear face of the wave. This feature and the known shift of microwave modulation to the forward face due to tilt effects explains the different observed phases of the microwave and IR modulation.

Collocated, simultaneous IR imagery and microwave Doppler spectra of breaking waves were compared for scales ranging from whitecaps to microbreakers. Consistent with previous investigations, the Doppler spectra corresponding to the whitecap exhibited peaks with large Doppler offset and a polarization ratio near unity. A notable result was that Doppler spectra for small- and micro-scale breaking waves exhibited similar characteristics. This result emphasizes the importance of including microscale wave breaking effects in models of microwave backscatter.

The laboratory experiment demonstrated that preferential microbreaking can be induced by swell waves. Furthermore, the laboratory results were consistent with our field result that microbreaking is initiated at or near the swell crest and the resulting T_{skin} maxima occurs on the rear face. That the phase of the modulation reported by JH disagreed with our field and laboratory results suggest that additional mechanisms such as enhanced wind stress or bound, tilted waves may play a role under wind and wave conditions significantly different from those we encountered.

Acknowledgment

We thank W. Keller and K. Hayes for assistance with the microwave measurements. We thank S. Long of NASA GSFC-WFF for use of the Air-Sea Interaction Research Facility and K. Phadnis and E. Lettvin for help with laboratory data collection.

[1] K. B. Katsaros, "The aqueous thermal boundary layer," *Bound.-Lay. Meteor.*, vol. 18, pp. 107-127, 1980.

[2] A. T. Jessup, C. J. Zappa, M. R. Loewen, and V. Hesany, "Infrared remote sensing of breaking waves," *Nature*, vol. 385, pp. 52-55, 1997.

[3] J. J. Simpson and C. A. Paulson, "Small-scale sea surface temperature structure," *J. Phys. Ocean.*, vol. 10, pp. 399-410, 1980.

[4] A. T. Jessup and V. Hesany, "Modulation of ocean skin temperature by swell waves," *J. Geophys. Res.*, vol. 101, pp. 6501-6511, 1996.

[5] J. H. Chang and R. N. Wagner, "Laboratory measurement of surface temperature fluctuations induced by small amplitude surface waves," *J. Geophys. Res.*, vol. 80, pp. 2677-2687, 1975.

[6] A. W. Miller, Jr. and R. L. Street, "On the existence of temperature waves a a wavy air-water interface," *J. Geophys. Res.*, vol. 83, pp. 1353-1365, 1978.

[7] G. A. Wick, A. T. Jessup, "Simulation of ocean skin temperature modulation by swell waves," *Journal of Geophysical Research,* vol. 101, pp. 6501-6511, Mar. 1996.

[8] W. C. Keller and W. J. Plant, "Cross sections and modulation transfer functions at L and Ku bands measured during the Tower Ocean Wave and Radar Dependence Experiment," *J. Geophys. Res.*, vol. 95, pp. 16277-16289, 1990.

[9] T. Hara and W. J. Plant, "Hydrodynamic modulation of short wind-wave spectra by long waves and its measurement using microwave backscatter," *J. Geophys. Res.*, vol. 99, pp. 9767-9784, 1994.

[10] R. Romeiser, A. Schmidt, and W. Alpers, "A three-scale composit surface model for the ocean wave-radar modulation transfer function," *J. Geophys. Res.*, vol. 99, pp. 9785-9801, 1994.

[11] T. Hara and W. J. Plant, "Hydrodynamic modulation of short wind-wave spectra by long waves and its measurement using microwave backscatter," *J. Geophys. Res.*, vol. 99, pp.9767-9784, 1994.

[12] W. J. Plant, "A model for microwave Doppler sea return at high incidence angles: Bragg scattering from bound, tilted waves," *J. Geophys. Res.*, vol. 102, pp. 21131-21146, 1997.

[13] M. L. Banner and O. M. Phillips, "On the incipient breaking of small scale waves," *Journal of Fluid Mechanics*, vol. 77, pp. 825-842, 1974.

[14] A. T. Jessup, C. J. Zappa, and H. Yeh, "Defining and quantifying microscale wave breaking with infrared imagery," *Journal of Geophysical Research*, vol. 102, pp. 23145-23153, 1997.

[15] C. J. Zappa, W. E. Asher, and A. T. Jessup, "Microscale wave breaking and air-water gas transfer," *Journal of Geophysical Research*, vol. 106, pp. 9385-9392, 2001.

[16] C. J. Zappa, W. E. Asher, A. T. Jessup, J. Klinke, and S. R. Long, "Microbreaking and the enhancement of air-water gas transfer velocities," *J. Geophys. Res.*, vol. 109, pp. doi:10.1029/2003JC001897, 2004.

[17] R. Fogelberg, "A Study of Microbreaking Modulation by Ocean Swell Using Infrared and Microwave Techniques," in *Dept. Civil Environ. Eng.*, vol. M.S. Seattle: Univ. Wash., 2003, pp. 129.

[18] C. J. Zappa, A. T. Jessup, and H. Yeh, "Skin layer recovery of free-surface wakes: Relationship to surface renewal and dependence on heat flux and background turbulence," *J. Geophys. Res.*, vol. 103, pp. 21711-21722, 1998.

[19] A. T. Jessup, W. Melville, and W. Keller, "Breaking waves affecting microwave backscatter 1. Detection and verification," *J. Geophys. Res.*, vol. 96, pp. 20547-20559, 1991.

[20] P. H. Y. Lee, J.D. Barter, K. L. Beach, C. L. Hindman, B. M. Lake, H. Rungaldier, J. C. Shelton, A. B. Williams, R. Yee, and H. C. Yuen, "X band microwave backscattering from ocean waves," *J. Geophys. Res.*, vol. 100, pp. 2591-2611, 1995.

[21] E. Ericson, D. Lyzenga, and D. Walker, "Radar backscatter from stationary breaking waves," *J. Geophys. Res.*, vol. 104, pp. 29679-29695, 1999.

[22] E. Dano, D. Lyzenga, and M. Perlin, "Radar backscatter from mechanically generated transient breaking waves - Part I: Angle of incidence dependence and high resolution surface morphology," *IEEE Trans. Geosci. Rem. Sens.*, vol. 26, pp. 181-200, 2001.

[23] M. Haller and D. Lyzenga, "Comparison of radar and video observations of shallow water breaking waves," *IEEE Trans. Geosci. Rem. Sens.*, vol. 41, pp. 832-844, 2003.

[24] S. R. Long, "NASA Wallops Flight Facility Air-Sea Interaction Research Facility," NASA Reference Publication no. 1277, 1992.

[25] P. M. Saunders, "The temperature at the ocean-air interface," *J. Atmos. Sci.*, vol. 24, pp. 269-273, 1967.

[26] G. A. Wick, W. J. Emery, L. H. Kantha, and P. Schluessel, "The behavior of the bulk-skin sea surface temperature difference under varying wind speed and heat flux," *J. Phys. Ocean.*, vol. 26, pp. 1969-1988, 1996.

[27] C. W. Fairall, E. F. Bradley, J. S. Godfrey, G. A. Wick, J. B. Edson, and G. S. Young, "Cool-skin and warm-layer effects on sea surface temperature," *J. Geophys. Res.*, vol. 101, pp. 1295-1308, 1996.

[28] C. J. Zappa, F A Tubiana, W R McGillis, J Bent, G De Leeuw, M M Moerman Investigating Wave Processes Important to Air-Sea Fluxes Using Infrared Techniques, AGU Ocean Sci. Mtg., Honolulu, HI, 2006.

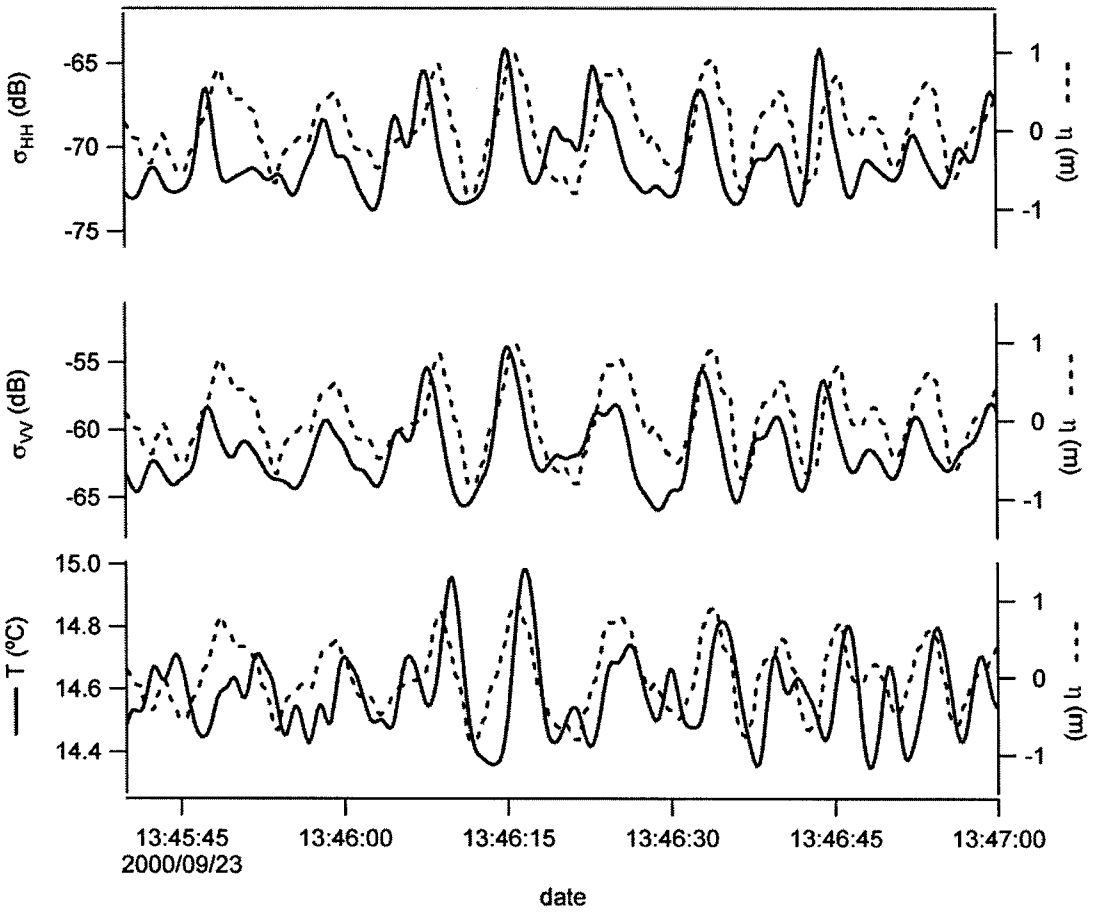

Fig. 1. Time series of field measurements showing coincident modulation of microwave cross section for VV and HH polariziations, (σ_{VV}, middle and σ_{HH}, top, respectively), and skin temperature (T_{skin}, bottom). The surface displacement, η, is repeated as a dashed line with each variable. In general, the T_{skin} maxima occur on the rear face while the σ maxima occur on the front face.

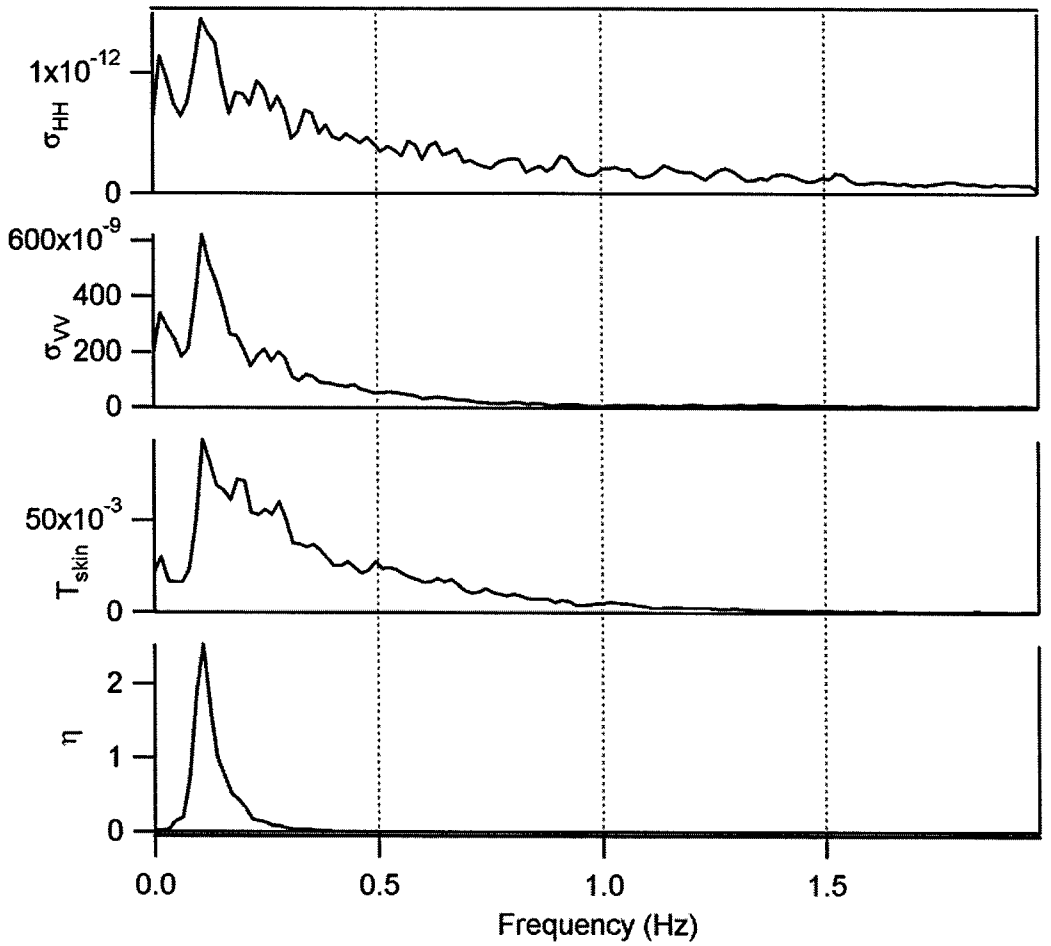

Fig. 2. Spectra of microwave cross sections, T_{skin}, and surface displacement all show a peak at the swell frequency.

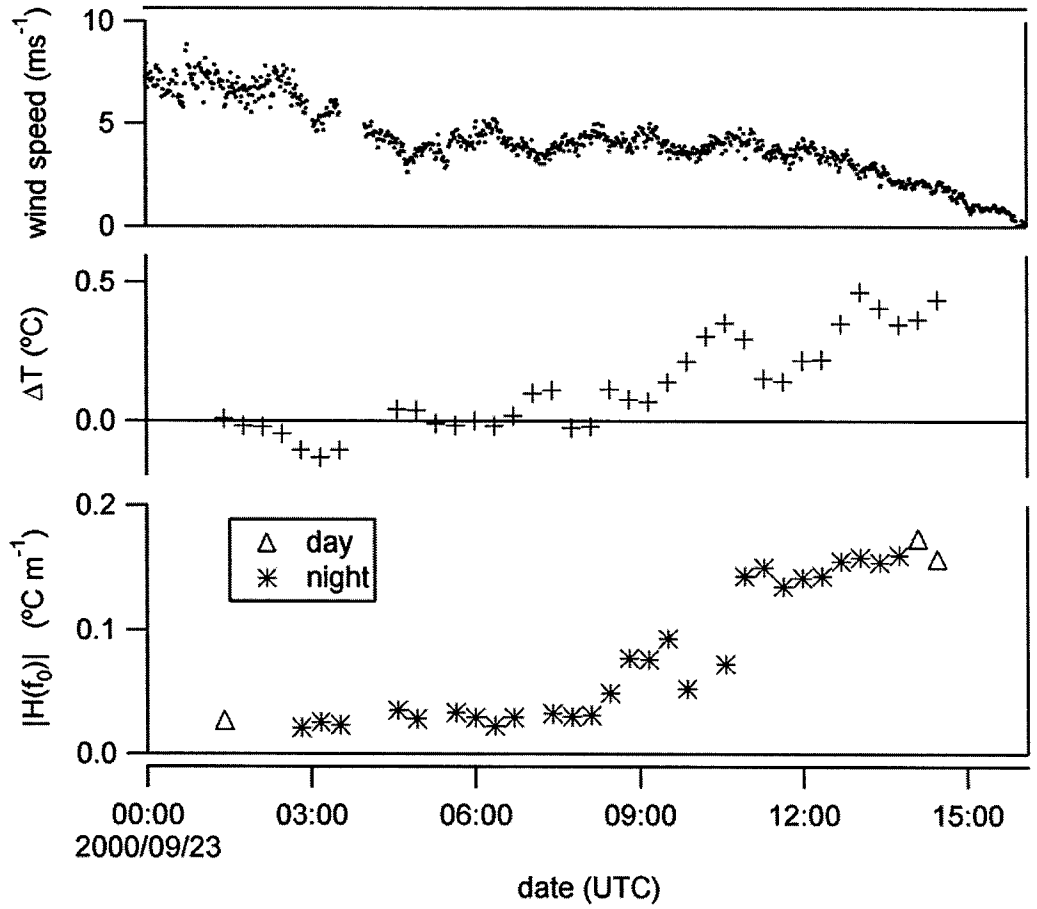

Fig. 3. Time series for the field measurements showing the dependence of the magnitude of the linear transfer function, $H(f_0)$, between T_{skin} and η.

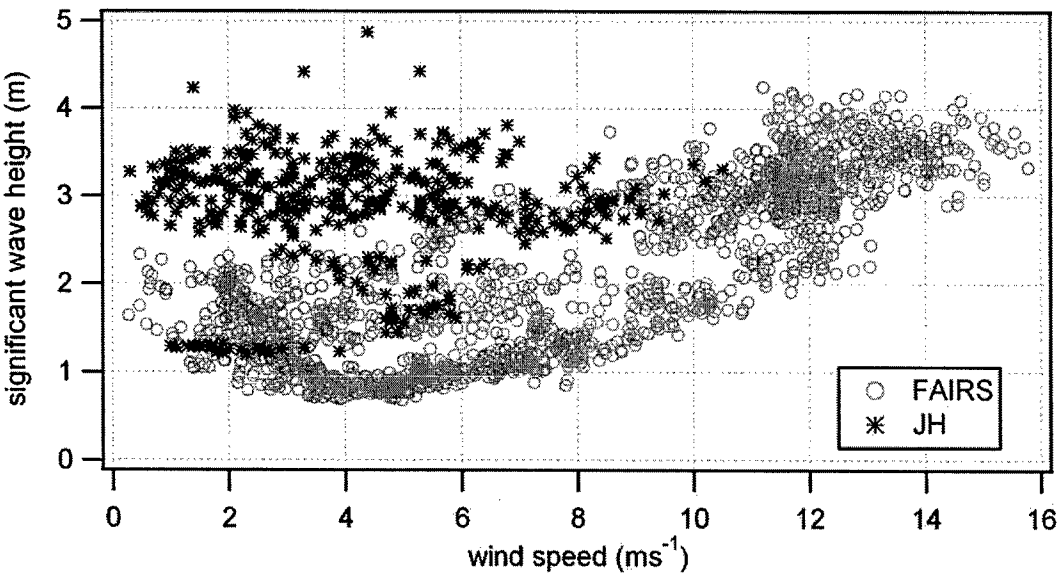

Fig. 4. Comparison of the significant wave height and the wind speed during the FAIRS Experiment and the JH measurements. The conditions of low wind speed and large wave height during the JH measurements resulted in large T_{skin} modulation, while the conditions during FAIRS resulted in relatively few cases of large T_{skin} modulation.

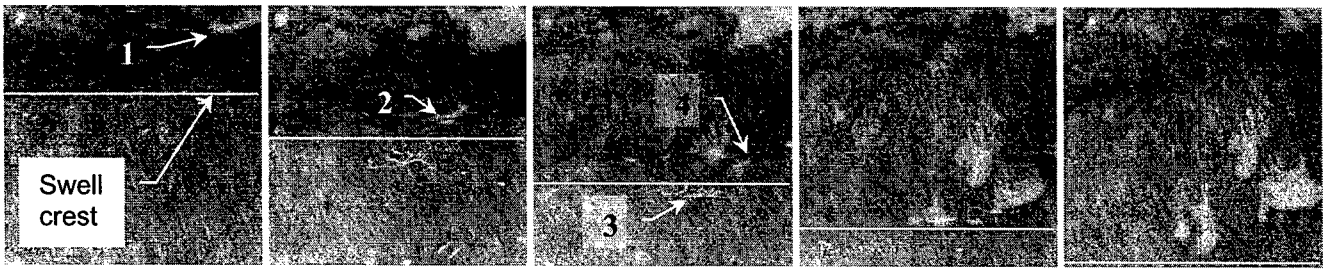

Fig. 5. Infrared image sequence of a swell wave crest propagating from top to bottom and causing microscale waves to break. Swell crest is marked as a white line and microbreakers are numbered where they first appear. Warmer temperatures appear white and cooler temperatures are dark showing an approximate 0.5°C temperature range. Time between images is 0.33 s and the images are approximately 4.8 m on a side. The breaking begins near the swell crest and the resulting warm wake is left behind to decay on the rear face.

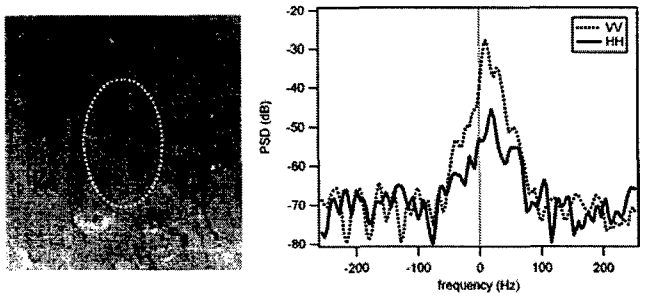
VV
HH
PSD (dB)
frequency (Hz)

(a)

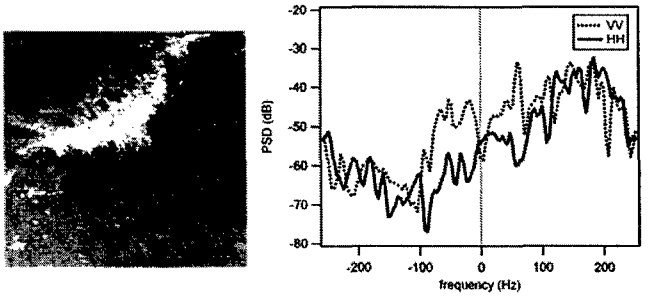
VV
HH
PSD (dB)
frequency (Hz)

(b)

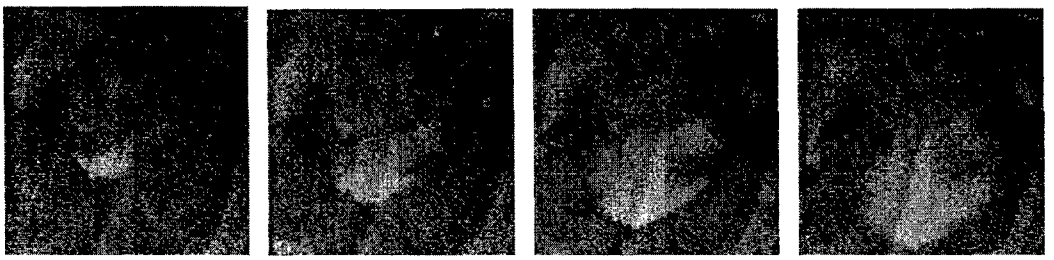

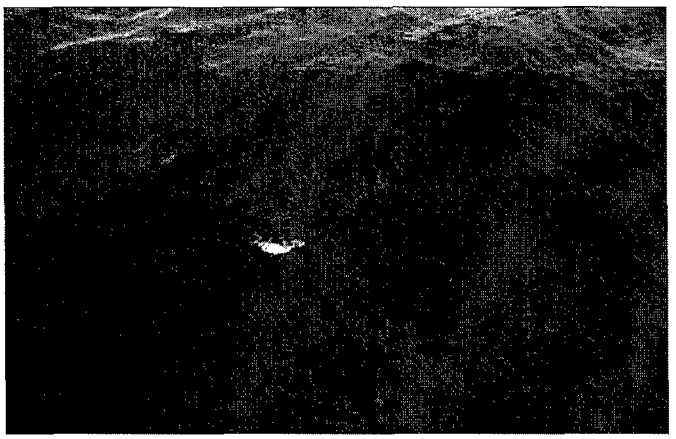

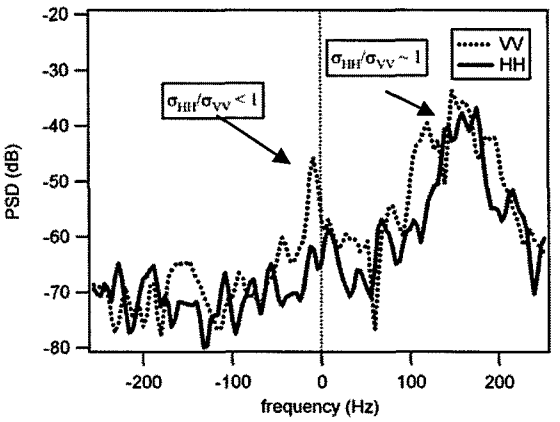
$\sigma_{HH}/\sigma_{VV} < 1$
$\sigma_{HH}/\sigma_{VV} \sim 1$
VV
HH
PSD (dB)
frequency (Hz)

(c)

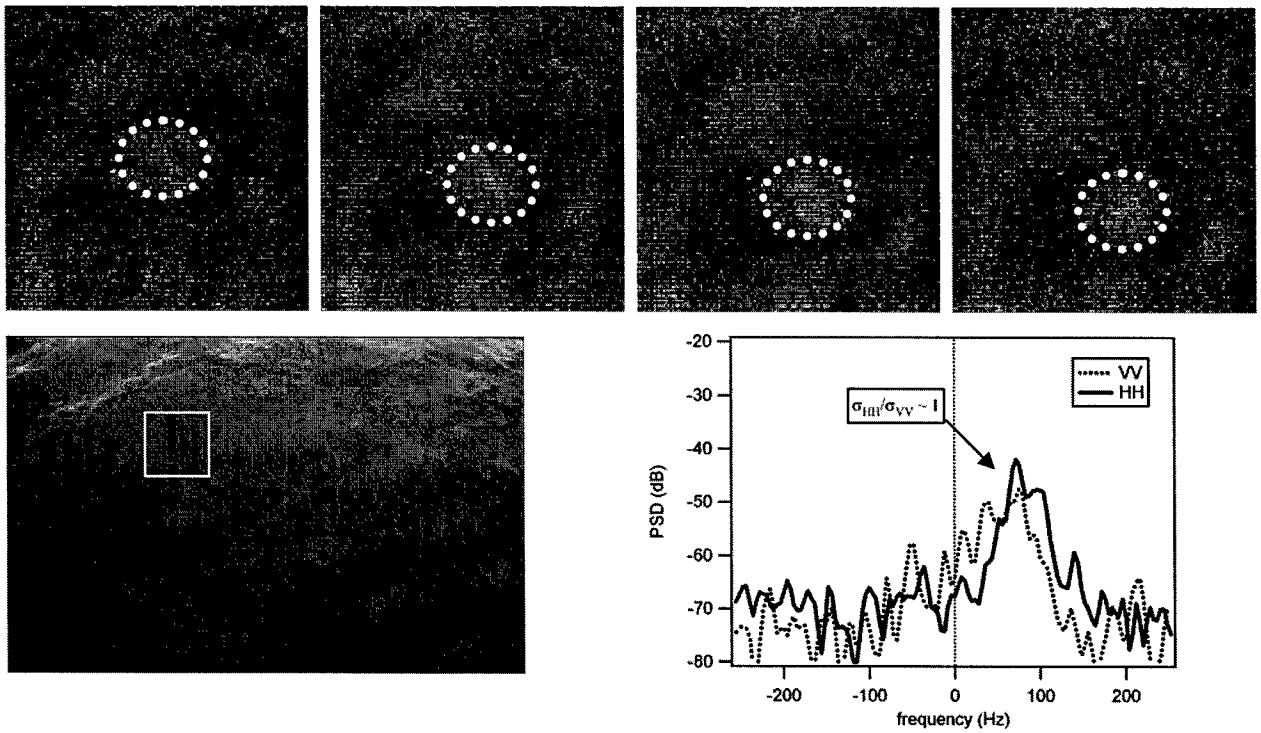

(d)

Fig. 6. Infrared imagery and microwave spectral signatures of different scales of breaking during FAIRS with wind speed 3.5 m s^{-1} and significant wave height of 0.75 m. (a) No breaking: spectra show small Doppler shift and $\sigma_{HH}/\sigma_{VV}<1$. The 3-dB spot is indicated by the dashed ellipse. (b) A large whitecap: spectra show large Doppler shift and $\sigma_{HH}/\sigma_{VV}\approx1$. (c) A small whitecap: visible in the accompanying video image, produces spectra with characteristics similar to those of the large whitecap. (d) A microscale breaking wave: the resulting wake is outlined by a dashed circle, has no visible signature in the video image (IR FOV is shown outlined in white). The spectra again show offset peaks with $\sigma_{HH}/\sigma_{VV}\approx1$. All infrared images are 4.8 m on a side except in (d) which are 1.2 m on side. Video images are 9.4 m x 14.8 m.

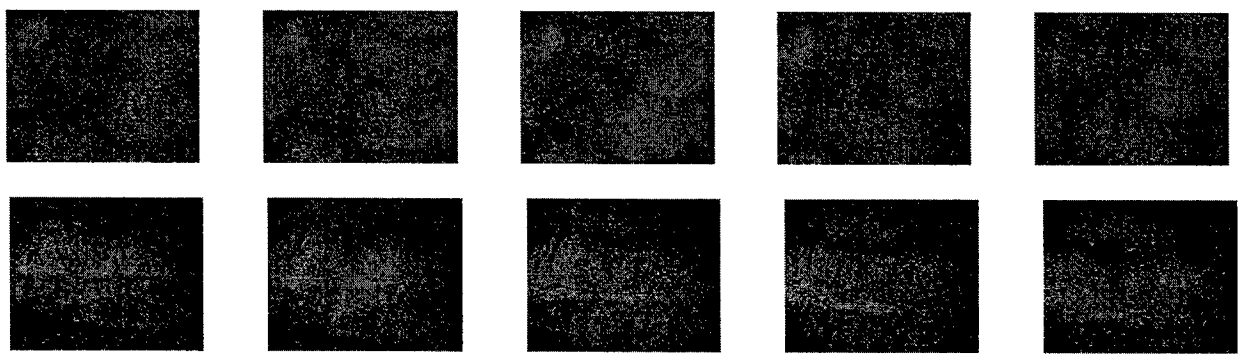

(a)

(b)

Fig. 7. Two infrared image sequences from the laboratory showing the difference in microscale breaking with (a) wind-waves only and (b) wind- and paddle-generated waves. In the case of wind waves only, the breaking appears to be randomly distributed. When both wind and swell waves are present, the microbreaking occurs preferentially near the swell crest, which appears as a warm band across the image. The time progresses from left to right and waves are propagating from top to bottom. The images are 64 by 80 cm and the time between images is 0.07 s. The wind speed was 5.5 m s^{-1}, the paddle frequency was 0.9 Hz, and the paddle-generated wave amplitude was 0.04 m.

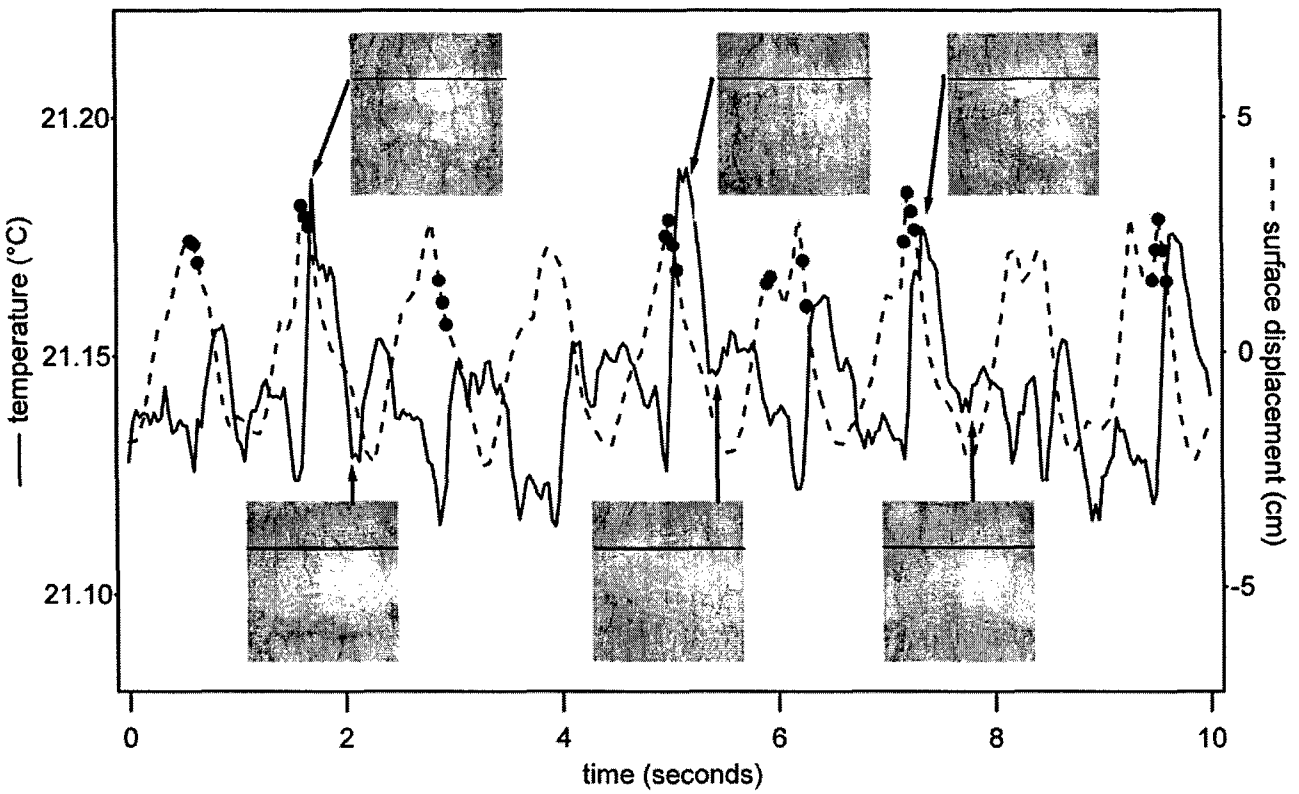

Fig. 8. Time series of temperature and surface displacement showing modulation of the temperature by swell waves in the laboratory. Black dots on the surface displacement time series show when microbreaker crests were detected passing the location of the wave gauge. Infrared images show the water surface at the time indicated by the arrows. The black line on the images shows the location of the pixels used to derive the skin temperature time series. The image pixel values were calibrated with a co-located IR radiometer. The breaking occurs at the swell crest but the temperature maxima from the wake occur on the rear face.